A truncated form of the p27 CDK inhibitor translated from pre-mRNA causes cell cycle arrest at G2 phase

Daisuke Kaida[a]*, Takayuki Satoh[a], Ken Ishida[a] and Rei Yoshimoto[b]

[a] Graduate School of Medicine and Pharmaceutical Sciences, University of Toyama, 2630 Sugitani, Toyama, 930-0194, Japan

[b] Department of Applied Biological Sciences, Faculty of Agriculture, Setsunan University, Hirakata, Osaka 573-0101, Japan

Corresponding author: Daisuke Kaida

Graduate School of Medicine and Pharmaceutical Sciences, University of Toyama, 2630 Sugitani, Toyama 930-0194, Japan

Tel/Fax: +81-76-415-8848

E-mail: kaida@med.u-toyama.ac.jp

Abstract

Pre-mRNA splicing is indispensable for eukaryotic gene expression. Splicing inhibition causes cell cycle arrest and cell death, which are the reasons of potent anti-tumor activity of splicing inhibitors. Here, we found that truncated proteins are involved in cell cycle arrest and cell death upon splicing inhibition. We analyzed pre-mRNAs accumulated in the cytoplasm where translation occurs, and found that a truncated form of the p27 CDK inhibitor, named p27*, is translated from pre-mRNA and accumulated in G2 arrested cells. Overexpression of p27* caused G2 phase arrest through inhibiting CDK-cyclin complexes. Conversely, knockout of p27* accelerated resumption of cell proliferation after washout of splicing inhibitor. Interestingly, p27* was resistant to proteasomal degradation. We propose that cells produce truncated proteins with different nature to the original proteins via pre-mRNA translation only under splicing deficient conditions to response to the splicing deficient conditions.

Introduction

More than 95% of protein-coding genes in humans consist of exons and intervening sequences, namely introns [1-3]. Introns are removed and exons are joined by pre-mRNA splicing to produce mature mRNA: the template for translation. Therefore, defects in splicing machineries cause accumulation of unspliced or partially spliced mRNAs. If such unspliced or partially spliced mRNAs are exported to the cytoplasm and translated into proteins, the proteins must have different amino acid sequences and might have different functions to the original proteins. Such proteins translated from pre-mRNA supposed to be non-functional or deleterious proteins that inhibit cellular functions [4] and might cause splicing related diseases [5-9]. To prevent translation from unspliced or partially spliced mRNAs, cells have multiple mRNA quality control mechanisms. The nuclear exosome degrades such unspliced mRNAs [10]. Even if unspliced mRNAs escape from degradation by the nuclear exosome, export of these mRNAs is strictly prohibited [11-13]. If unspliced and partially spliced mRNAs leak from the nucleus, they are degraded by nonsense-mediated mRNA decay (NMD) in the cytoplasm [14]. These mRNA quality control mechanisms prevent production of non-functional proteins translated from pre-mRNAs and protect the integrity of the proteome.

Splicing inhibitors, including spliceostatin A (SSA) and pladienolide B (Pla-B), cause G1 and G2/M phase arrest and cell death [15-18]. Such cell cycle arrest and cell death are thought to be the reasons of the anti-tumour activity of the splicing inhibitors. We previously investigated the molecular mechanism of the cell cycle arrest induced by splicing inhibition and found that upregulation of the cyclin-dependent kinase (CDK) inhibitor p27 and a C-terminus truncated form of p27, named p27*, is one of the causes of G1 phase arrest induced by splicing inhibition [19]. Interestingly, p27* is translated from pre-mRNA of the *CDKN1B (p27)* despite mRNA quality control mechanisms [15]. In

addition, we found that downregulation of cyclin E1, cyclin E2 and E2F1 is another cause of G1 phase arrest induced by splicing inhibition [20]. However, it is still totally unknown how splicing-deficient cells arrest at G2/M phase.

Cell cycle progression is tightly regulated by the kinase activity of CDK-cyclin complexes [21,22]. Among CDKs and cyclins, Cdk1 (also known as Cdc2), cyclin A, and cyclin B are critical regulators of G2/M phase [23-25]. The kinase activity of Cdk-cyclin complexes is regulated by several mechanisms. The protein levels of cyclins A and B oscillate during the cell cycle. Cyclin A starts accumulating in S phase and suddenly decreases at early M phase [26-30]. Cyclin B starts accumulating in G2 phase and decreases at late M phase [24,31-33]. Because cyclin A and B proteins are required for Cdk1 activity, the Cdk1 activity is proportional to the amount of the cyclin proteins. In addition to the amount of the cyclin proteins, the phosphorylation status of Cdk1 regulates Cdk1 activity. Cdk1 is phosphorylated at Thr14 and Tyr15 residues in G2 phase and the phosphorylation negatively regulates Cdk1 kinase activity [24,34,35]. At the end of G2 phase, Cdk1 is dephosphorylated by Cdc25C for activation, and consequently cells enter M phase [24,36]. In addition to the above two mechanisms, it is well known that CDK inhibitor proteins negatively regulate the kinase activity of Cdk-cyclin complexes [22,37]. As mentioned above, p27 is such a CDK inhibitor that controls G1/S transition [38]. In fact, p27 is highly expressed in G0/G1 phase and degraded by the ubiquitin-proteasome pathway from S to M phase [39,40]. Therefore, p27 does not appear to control G2/M transition under physiological conditions. However, interestingly, knockout of Skp2, which is a component of SCF (Skp, Cullin, F-box containing complex) ubiquitin ligase for p27 ubiquitylation, causes accumulation of p27 in G2 phase. The accumulated p27 inhibits M phase cyclins and consequently causes G2 arrest [40].

In this study, we found that splicing inhibition causes cell cycle arrest and subsequent cell death, and that truncated proteins translated from pre-mRNA contributes to the phenotypes. Furthermore, we revealed that p27*, which inhibits M-phase cyclin and resistant to proteasomal degradation, is the key factor for the G2 phase arrest upon splicing inhibition.

Results

Splicing inhibition causes cell cycle arrest and cell death

To understand the molecular mechanisms of cell cycle arrest and cell death upon splicing inhibition, we treated HeLa S3 cells with Pla-B and investigated the cell proliferation. Compared with MeOH (the vehicle for Pla-B), 1 ng/ml Pla-B partially inhibited cell proliferation and >2 ng/ml Pla-B completely suppressed cell proliferation (Fig. 1A). We analysed cell viability and found that Pla-B treatment had little effect on the cell viability until 24 h and then caused cell death at 48 h and 72 h (Fig. 1B). We also investigated when apoptosis starts to occur in Pla-B treated cells. To this end, we tested if cleavage of poly(ADP-ribose) polymerase (PARP) is observed in Pla-B treated cells, because cleaved PARP is a useful hallmark of apoptosis [41]. We observed PARP cleavage in Pla-B–treated cells at 48 h and 72 h, but not at 24 h, which is consistent with the result above (Fig. 1A, 1B, S1A). It is well known that the p53 tumour suppressor, which is a key factor for apoptosis and cell cycle arrest, is barely expressed in HeLa S3 cells because of its quick degradation[42-44]. It is possible that such low expression of p53 affects the timing of the onset of apoptosis and cell cycle arrest. To test the hypothesis, we performed the same experiments using breast cancer cell lines: MDA-MB-231 cells and MCF7 cells harboring mutant p53 and wild-type p53, respectively. We observed no conspicuous difference of cell proliferation, cell viability and PARP cleavage upon Pla-B treatment

between the two cell lines, suggesting that Pla-B treatment causes cell cycle arrest at first, then cell death regardless of existence of wild-type p53 (Fig. S1B-D).

If the cell cycle arrest and cell death are caused by splicing inhibition, cell proliferation should resume after removal of Pla-B, because Pla-B binds to its target protein, SF3B1, non-covalently [45]. To test the hypothesis, cells were treated with 3 or 10 ng/ml Pla-B, after which Pla-B was washed out. After washout following Pla-B treatment for 2 h, cell proliferation resumed and almost no dead cells were observed, suggesting that cell cycle progression was arrested only under splicing-deficient conditions (Fig. 1C). Interestingly, however, after washout following Pla-B treatment for 8 h, resumption of cell proliferation was delayed (Fig. 1C). After treatment for 12, 16, and 24 h, the cells did not grow and cell death was observed at 48 h and 72 h in spite of the Pla-B washout (Fig. 1C, 1D). We speculated that splicing activity was not restored even after Pla-B washout. To test the hypothesis, we assessed splicing activity in the cells by measuring the relative expression levels of exon-exon junction and adjacent exons. We found that splicing activity was recovered after washout of Pla-B (Fig. 1E, Fig. S2A, S2B). To note that, the relative expression level of *SMEK2* Ex5 was much smaller than that of *SMEK2* Ex3 (Fig. S2B), which is consistent with previous results indicating that transcription elongation of the *SMEK2* gene is inhibited by splicing inhibition[46-48]. In addition, we investigated if SF3B1 is phosphorylated after Pla-B washout, because SF3B1 is phosphorylated only in the active spliceosome [49,50]. We found that SF3B1 was phosphorylated in the control cells and Pla-B washout cells, but not in the Pla-B treated cells (Fig. 1F). This result also indicate that splicing activity was recovered after washout of Pla-B. After washout following 10 ng/ml Pla-B treatment for 16 and 24 h, SF3B1 was not phosphorylated. In such cells, Pol II protein level was substantially lower than control cells, and transcription did not appear to occur, consequently active splicing might not have occurred (Fig. 1F, S2A) Therefore, we could not observe phosphorylated SF3B1 in such cells. Taken together, we observed cell cycle arrest and cell death

even after washout of Pla-B, but splicing activity was recovered in such cells. Therefore, we speculated that other mechanisms than decrease in gene expression of cell cycle regulators caused by splicing inhibition contribute to the cell cycle arrest and cell death.

Truncated proteins translated from pre-mRNA contribute to cell death and cell cycle arrest

To understand the molecular mechanism of cell cycle arrest and cell death in Pla-B treated cells, we compared the effect of Pla-B with transcription inhibitor actinomycin D (Act D), or translation inhibitor cycloheximide (CHX) to inhibit gene expression through different mechanisms. All compounds inhibited cell proliferation (Fig. 2A). Pla-B caused cell death at 48 and 72 h consistent with the result above (Fig. 2B). Act D appeared more toxic than Pla-B, but CHX did not induced apparent cell death even at 72 h (Fig. 2B). These results suggest that CHX induces cell cycle arrest, but not cell death. Next, we compared the effect of CHX and Pla-B on cell cycle progression and found that both Pla-B and CHX caused G2/M phase arrest, but the percentage of G2/M phase-arrested cells caused by Pla-B was significantly higher than that of CHX-treated cells (Fig. 2C). Because Pla-B and CHX inhibit gene expression but Pla-B caused cell death and G2/M phase arrest more prominently than CHX, Pla-B specific mechanism appeared to cause G2/M phase arrest and cell death. We assumed that truncated proteins which are translated from pre-mRNA contribute to these phenotypes, and if this is the case, CHX treatment could suppress the effects of Pla-B by inhibiting the production of such truncated proteins. To investigate the hypothesis, we treated the cells with CHX and Pla-B simultaneously and found that CHX treatment indeed suppressed the cell death and G2/M phase arrest caused by Pla-B treatment (Fig. 2D and 2E), suggesting that truncated proteins translated from pre-mRNA function to cause G2/M phase arrest and cell death.

Low and high concentrations of Pla-B cause M phase and G2 phase arrest respectively

In this study, we decided to investigate the molecular mechanism of G2/M phase arrest caused by Pla-B treatment. First, we analysed the effect of Pla-B on cell cycle progression after cell cycle synchronization by a double thymidine block. We found that >2 ng/ml Pla-B treatment caused G2/M phase arrest by measuring the DNA content of each cell, although 1 ng/ml Pla-B caused partial cell cycle arrest (Fig. 3A, 3B, Fig. S3). Pla-B-treated cells showed an almost identical pattern to control cells until 8 h, suggesting that Pla-B treatment did not affect S phase progression under these experimental conditions, which is consistent with the previous report [16] (Fig. 3B and S3).

We also investigate the cell morphology of Pla-B treated cells, because DNA contents of G2 and M phase cells are the same, therefore we could not distinguish G2 phase cells from M phase cells based on their DNA content. To this end, we observed cell morphology and counted the number of round cells, a feature of M phase cells [51]. The proportion of round cells among MeOH-treated cells was approximately 40% at 10 h and then decreased (Fig. 3C). Pla-B at 1 ng/ml caused accumulation of round cells at 14 h and then the proportion decreased gradually, but ~30% of cells maintained their round shape (Fig. S4). Upon 2 or 3 ng/ml Pla-B treatment, round cells had accumulated at 20–36 h (Fig. 3C, S4). In contrast, upon 5 ng/ml Pla-B treatment, most cells were flat until 24 h, and >7 ng/ml Pla-B treated cells were flat until 36 h (Fig. 3C, S4). These results suggested that low concentrations of Pla-B caused M phase arrest and high concentrations of Pla-B caused G2 phase arrest.

In addition to the DNA content and cell morphology, we analysed protein levels of cell cycle regulators by immunoblotting upon Pla-B treatment (Fig. 3D and S5). Degradation of cyclin A2, which is a hallmark of M phase entry, was delayed in 2 or 3 ng/ml Pla-B-treated cells [26,28], and no degradation of cyclin A2 was observed in higher concentrations of Pla-B treated cells (Fig. 3D and S5), suggesting that low concentration of Pla-B causes delay of G2/M transition, and higher concentration of Pla-B causes inhibition of G2/M transition. Cyclin B1, which is degraded at late M phase (anaphase) [24,31-33], was stable in >2 ng/ml Pla-B treated cells (Fig. 3D and S5), suggesting that

lower concentration of Pla-B causes cell cycle arrest before anaphase. We also examined the phosphorylation status of Cdk1 Y15, which is dephosphorylated at the end of G2 phase and its dephosphorylation is required for activation of Cdk1 and G2/M transition [36,52]. Dephosphorylation of Cdk1 Y15 was delayed in 2 or 3 ng/ml Pla-B-treated cells, and no dephosphorylation of CDK1 Y15 was observed in higher concentrations of Pla-B treated cells (Fig. 3D and S5). These results supported the idea that low concentrations of Pla-B caused M phase arrest and high concentrations of Pla-B caused G2 phase arrest, which is consistent with the above results (Fig. 3B, 3C, S3-S5).

p27* is accumulated in G2 phase arrested cells

Above reslts indicated that truncated protein contributes to G2/M phase arrest (Fig. 2). To seek a truncated protein which is responsible for the G2/M phase arrest by splicing inhibition, we utilized our previous data [53]. For production of a truncated protein from pre-mRNA, the pre-mRNA should be accumulated in the cytoplasm where translation occur. In our previous report, we found that splicing pattern of 87 introns are affected in the cytoplasm after splicing inhibition [53]. Out of the introns, we picked up 13 introns based on the gene ontology analysis and the length of estimated truncated protein (Table S1). We performed RT-PCR to investigate if the 13 introns are accumulated in Pla-B treated cells and found that 3 introns: *RGS2 Ex1- Int4*, *TBX3 Ex1-Int1* and *CDKN1B Ex1-Int1* (p27*) were highly accumulated in Pla-B treated cells (Fig. S6). We cloned cDNAs to construct expression plasmids of the truncated forms of Rgs2 and Tbx3 and confirmed expression of the truncated proteins (Fig. S7A). Because we already constructed the p27* expression plasmid [19], we reconfirmed its expression (Fig. S7B). In addition, if antibodies which recognize the N-terminus of truncated proteins are commercially available, we investigated whether endogenous truncated proteins are produced or not in Pla-B treated cells. As a result, we found that only p27* could be detected but not Wee1 and Plk2 truncated forms (Fig. S7C). Next, we assessed the effect of

overexpression of Rgs2 truncated protein, Tbx3 truncated protein and p27* on cell cycle proliferation and cell viability, and found that only p27* inhibited cell proliferation, although p27* did not affect cell viability (Fig. S7D and E). These results suggest that p27* is the responsible truncated protein for G2 phase arrest caused by splicing inhibition. If so, p27* should be accumulated in G2 arrested cells caused by splicing inhibition. Indeed, p27* was accumulated in the high-concentration Pla-B-treated cells which were arrested in G2 phase (Fig. 3D and S5).

Overexpression of p27* causes G2 phase arrest

As mentioned above, p27* was accumulated in the G2 arrested cells. Next, we tested whether p27* induces G2 phase arrest. To this end, we established a stable cell line expressing Flag-p27* with expression controlled by a tetracycline-responsive promoter. We confirmed p27* expression only in doxycycline (DOX) treated cells (Fig. 4A). We observed partial G2/M phase arrest of DOX treated cells, suggesting that p27* overexpression causes G2/M phase arrest (Fig. 4B). We also investigated the expression levels of cyclin A2 in DOX-treated cells. Cyclin A2 was still observed from 14 to 20 h in DOX-treated cells (Fig. 4A), suggesting that a proportion of the Flag-p27* expressing cells was arrested at early M phase, because cyclin A2 is degraded at the end of G2 phase [26,28]. Furthermore, we observed the morphology of the cells at 20 h and found that only ~5% of the cells were round. This result also indicates that most of the arrested cells were arrested in G2 phase, but not in M phase (Fig. 4C).

If accumulation of p27* is the only cause of the G2 phase arrest induced by splicing inhibition, knockdown of p27* should rescue the G2 phase arrest. To test this hypothesis, we utilized an siRNA against *CDKN1B* to knockdown p27*. Knockdown of p27* was confirmed by immunoblotting (Fig. 4D). At 8 h, most cells were in G2/M phase regardless of treatment with the siRNA and Pla-B (Fig. 4E). Without Pla-B treatment, most cells transitioned to G1 phase at 12 h

with or without siRNA treatment. Upon Pla-B treatment, the majority of cells were arrested in G2/M phase, which is consistent with the above results (Fig. 3). However, even after p27* knockdown, the cells were still arrested in G2/M phase at 12 h. In addition, we observed the cell morphology and found that only ~10% of the cells were round at 12 h (Fig. 4F), suggesting that these cells were arrested in G2 phase, but not M phase. Therefore, p27* knockdown could not rescue the G2 phase arrest caused by splicing inhibition and presumably downregulation of gene expression of cell cycle regulators also contribute to the G2 phase arrest caused by splicing inhibition.

p27* binds to and inhibits M phase Cyclins

Because p27* caused partial G2 phase arrest (Fig. 4), we invesitigaed if p27* inhibits the kinase activity of M phase cyclins: Cdk1-cyclin A and Cdk1-cyclin B complexes. To inviestigate whether p27* bound to M phase cyclins, we performed immunoprecipitation experiments. Flag-p27* was precipitated using a mouse anti-Flag antibody, and Cdk1 and cyclin B1 were coimmunoprecipitated with Flag-p27* (Fig. 5A, left panel). Because the molecular weights of cyclin A2 and the heavy chain are almost the same, we could not confirm the binding between cyclin A2 and p27*. To confirm the binding, we also performed immunoprecipitation using a rabbit anti-Flag antibody and found that cyclin A2 was coimmunoprecipitated with p27* (Fig. 5A, right panel).

To investigate whether p27* inhibits the kinase activity of the CDK-cyclin complexes, we performed an *in vitro* kinase assay. Flag-tagged p27 full-legth (hereafter called p27 FL) and Flag-p27* were purified and successful purification of the proteins was confirmed by oriole staining and immunoblotting (Fig. S8). Both p27 FL and p27* inhibited the kinase activity of recombinant Cdk1/cyclin A2 and Cdk1/cyclin B1 in a dose-dependent manner (Fig. 5B, 5C). These results suggest that p27* binds to and inhibits M phase cyclins.

p27* is resistant to proteasomal degradation

To investigate why only p27*, but not p27 FL, was observed in G2 arrested cells, we examined the splicing pattern of the *CDKN1B* gene. If splicing of *CDKN1B* pre-mRNA is completely inhibited and spliced mRNA does not exist, p27 FL protein, which is translated from spliced mRNA, cannot be produced. We tested this hypothesis, but both spliced and unspliced forms of *CDKN1B* mRNA were observed in the cells, suggesting that both p27 FL and p27* proteins were produced in Pla-B-treated cells (Fig. 6A). Next, we focused on the difference between the C-terminus resions of p27 FL and p27*. In the C-terminus of p27 FL, there is a phosphorylation site (threonine 187), and phosphorylation of the site is the trigger for ubiquitylation and proteasomal degradation [54]. This mechanism keeps the p27 FL protein level low in G2/M phase. Because p27* is a C-terminus-truncated form, p27* lacks the phosphorylation site [15]. To investigate whether p27* escapes proteasomal degradation, we checked expression level of Flag-p27 FL and Flag-p27* in G2/M phase by synchronizing cell cycle of Flag-p27 FL- and Flag-p27*-expressing cells. Treatment with MG132, a potent proteasome inhibitor, increased the amount of Flag-p27 FL, suggesting that Flag-p27 FL was degraded by the proteasome in G2/M phase (Fig. 6B), which is consistent with the previous report [40]. However, the amount of Flag-p27* was not increased by MG132 treatment, but slightly decreased by an unknown mechanism. We also investigated proteasomal degradation of endogenous p27 FL and p27*. The cell cycle of HeLa cells was synchronized, and the cells were treated with Pla-B and MG132. We found that the amount of endogenous p27 FL was increased by MG132 treatment, but not p27*, suggesting that endogenous p27* is also resistant to proteasomal degradation (Fig. 6C). Because p27* does not have the phosphorylation site for ubiquitylation, we compared the ubiquitylation levels of p27 FL and p27*. To check the ubiquitylation level, HEK293T cells were transfected with Flag-p27 FL, Flag-p27*, or vector plasmids. To observe ubiquitylation of p27 FL and p27* clearly, the cells were treated with MG132 and transfected with the HA-Skp2 plasmid [55],

because Skp2 protein recruits p27 to SCF ubiquitin ligase. Ubiquitylated proteins were purified from the cells by tandem ubiquitin-binding entity (TUBE) [56] and analysed by immunoblotting (Fig. 6D). We observed stronger signals of higher molecular weight bands of Flag-p27 FL than Flag-p27*. This result indicates that p27* was less ubiquitylated than p27 FL, presumably because p27* lacks the phosphorylation site to trigger ubiquitylation. Taken together, these results suggest that p27 FL was degraded by the ubiquitin-proteasome pathway in G2/M phase, but p27* was resistant to degradation, consequently only p27* was accumulated at G2/M phase in Pla-B-treated cells.

Because p27* was highly stable, p27* might remain in the Pla-B washout cells and such remaining p27* might contribute to the cell cycle arrest after washout of Pla-B (Fig. 1). To test the hypothesis, we investigated the p27* protein level after Pla-B treatment followed by washout (Fig. 6E). As we expected, p27* was still observed even at 72 h. Next, to investigate the effect of remaining p27* on cell proliferation, we utilized p27/p27* KO cells [20]. Although proliferation of both wild-type and p27/p27* KO cells resumed after Pla-B washout, the recovery of proliferation of p27/p27* KO cells was faster than wild-type cells statistically significantly (Fig. 6F). These results suggest that the highly stable truncated protein p27*, which is translated from pre-mRNA, contributes to the cell cycle arrest.

Discussion

Pre-mRNA splicing is one of the most important mechanisms for the transcriptome integrity and proteome integrity in eukaryote. Abnormalities in this process might cause production of aberrant, non-functional proteins translated from pre-mRNA, which might inhibit functional proteins. To prevent the production of such abnormal proteins, cells have several mRNA quality control mechanisms [10-14]: pre-mRNA degradation by the nuclear exosome, nuclear retention of pre-mRNA, and degradation of unspliced and partially spliced mRNAs by NMD. However, in this study, we

found that such a truncated protein, p27*, was produced only under splicing deficient conditions. Why can p27* be produced nevertheless the mRNA quality control mechanisms prevent pre-mRNA translation? We reported that very few selected pre-mRNAs with introns are accumulated in the cytoplasm under splicing-deficient conditions[53]. This finding indicates that the mRNA quality control mechanisms indeed prevent accumulation of most of pre-mRNAs in the cytoplasm undersplicing deficient conditions. Exceptionally, *CDKN1B (p27)* pre-mRNA appeared to escape from the mRNA quality control mechanisms. We have revealed that short pre-mRNAs with weak 5' splice site tend to escape from the nuclear retention mechanism [53]. Because *CDKN1B* pre-mRNA (5.2 kb) is much shorter than the average length of human genes (27 kb) [57], *CDKN1B* pre-mRNA might be able to escape from the retention mechanism. Once p27* is produced, p27* appeared to remain for a long while. In this study, we observed that p27* is resistant to proteasomal degradation, presumably because p27* does not possess the phosphorylation site, whose phosphorylation is the trigger for ubiquitination from S to M phase [54]. Therefore, p27* is highly stable compared with p27 FL. Furthermore, another feature might make p27* a stable protein. p27 FL consists of 198 amino acids and exon 1 of *CDKN1B* encodes 158 amino acids out of the 198 amino acids [15]. Most part of p27* is identical to p27 FL. Therefore p27* does not appear to be a short peptide, but a stable protein. In addition to stability, the high identity between p27* and p27 FL gives p27* a physiological function. The CDK inhibitory domain of p27 resides in the N-terminus of p27 [37], which is also included in p27*. As a consequence, p27* has the same potent CDK inhibitory activity as p27 FL. Taken together, these natures of *CDKN1B* pre-mRNA and p27* protein make p27* a stable protein with a physiological function.

So, why do cells produce p27* under splicing deficient conditions? We speculate that the *CDKN1B* gene functions as a sensor for splicing abnormalities. Transcriptome and proteome are perturbated in

splicing deficient cells, and such perturbation might cause splicing related diseases including myelodysplastic syndromes and leukaemia [5-9]. Therefore, proliferation of splicing deficient cells might increase the risk of such splicing related diseases. To reduce the risk, proliferation of splicing deficient cells should be inhibited. To inhibit proliferation of splicing deficient cells, p27* is a suitable protein, because p27*, a stable protein with cell cycle inhibitory activity, is translated from pre-mRNA only under splicing deficient condition. We assume that this system protects our body from splicing abnormality by minimizing the effect of splicing deficient cells to out body. We also speculate that there are other truncated proteins translated from pre-mRNA to adapt to splicing deficient conditions. Indeed, we found that another truncated protein appeared to contribute to cell death upon Pla-B treatment in this study. We will reveal the entire molecular mechanism that cells adapt to splicing deficient conditions utilizing truncated proteins in a future study.

The system that truncated proteins inhibit cells proliferation can be embraced for tumor suppression. If we inhibit splicing of cancer cells, cell proliferation of cancer cells should be inhibited by the truncated proteins and downregulation of gene expression. Indeed, Pla-B and SSA have been reported as potent anti-tumour reagents [15-18,58,59]. Although a phase I clinical trial of E7017, a derivative of Pla-B, was discontinued because of serious side effects [60], H3B-8800, another Pla-B derivative, has been investigated in a phase 1/2 study [59,61]. So far, the compound has been developed for myelodysplasia, acute myelogenous leukaemia, and chronic myelomonocytic leukaemia patients with spliceosome mutations. This study and future studies regarding truncated proteins translated from pre-mRNA might contribute to development of a novel anti-tumour reagent with less side-effects that targets broad types of cancer.

In this study, we found that is produced from pre-mRNA in splicing-deficient cells and inhibits cell cycle progression through binding to and inhibiting M phase cyclins. We believe that these findings may contribute to further understanding of the mechanisms that protect our body from splicing abnormality and the development of novel anti-cancer drugs based on splicing inhibitors.

Materials and Methods

Cell culture and synchronization

HeLa S3, HEK293T, MCF7 and MDA-MB-231 cells were cultured in Dulbecco's modified Eagle's medium containing 10% heat-inactivated fetal bovine serum (Thermo Fisher Scientific, Waltham, MA, USA). Cells were maintained in 5% CO_2 at 37°C. For cell cycle synchronization, the cells were treated with 2 mM thymidine (FUJIFILM Wako Pure Chemical Corporation, Osaka, Japan) for 18 h. After treatment, the cells were washed twice with phosphate-buffered saline (PBS) to release from the thymidine block and then cultured in fresh culture medium for 8 h. The cells were treated with 2 mM thymidine again for 16 hours and then washed with PBS twice to release from the double thymidine block.

Antibodies and reagents

A mouse monoclonal anti-α-tubulin antibody (T6074) was purchased from Sigma-Aldrich (St. Louis, MO, USA). Mouse monoclonal anti-Cyclin A2 (#4656), rabbit polyclonal anti-Cyclin B1 (#4138), mouse monoclonal anti-cdc2 (#9116), rabbit polyclonal anti-phospho-cdc2 (Tyr15) (#9111), mouse monoclonal anti-Cyclin E1 (#4129), rabbit monoclonal anti-Plk2 (#14812), rabbit monoclonal anti-Wee1 (#13084) and rabbit monoclonal anti-p27 (#3686) antibodies were purchased from Cell Signaling Technology (Danvers, MA, USA). Mouse monoclonal anti-RNA polymerase II (8WG16) was purchased from BioLegend (San Diego, CA, USA). Mouse monoclonal anti-Sap155 (D-221-3),

mouse monoclonal anti-Myc (My3), mouse monoclonal anti-DDDDK (FLA-1) and rabbit polyclonal anti-DDDDK (PM020) antibodies were purchased from Medical and Biological Laboratories (MBL) (Nagoya, Japan). Rabbit polyclonal anti-PARP-1 (H-250) antibody was purchased from Santa Cruz Biotechnology (Santa Cruz, CA, USA). HRP-conjugated anti-mouse IgG and anti-rabbit IgG secondary antibodies were purchased from GE Healthcare (Chicago, IL, USA). Doxycycline, puromycin, and G418 were purchased from TaKaRa Bio (Shiga, Japan). Pladienolide B was purchased from Santa Cruz Biotechnology. MG132, actinomycin D, and cycloheximide were purchased from Sigma-Aldrich.

Cell count and cell viability assay

After trypsinization, the numbers of viable and dead cells were counted using trypan blue exclusion and a hemocytometer.

Cell cycle analysis

Cells were fixed in 70% ethanol, rinsed with PBS, and then stained with a solution containing 20 μg/ml propidium iodide (Thermo Fisher Scientific), 0.05% Triton X-100, and 0.1 mg/ml RNase A (Thermo Fisher Scientific). The cell cycle was monitored by the image-based cytometer Tali (Thermo Fisher Scientific).

Morphological observation

Cells were synchronized using thymidine and treated with Pla-B. Morphology of the cells was then observed under an IX73 microscope (Olympus, Tokyo, Japan).

RNA preparation and RT-PCR

Total RNA was extracted from cells using TRIzol reagent (Thermo Fisher Scientific), following the manufacturer's instructions. cDNA was prepared using Primescript Reverse Transcriptase (TaKaRa Bio) and random primers. PCR was performed using TaKaRa ExTaq (TaKaRa). PCR products were analysed using a 1% agarose gel. To measure splicing activity, we purified nascent RNA using the Click-iT Nascent RNA Capture Kit (Thermo Fisher Scientific). Briefly, cells were treated with 200 μM of 5-ethynyl-uridine for 1 h, and total RNA was extracted from cultured cells using TRIzol reagent. Labeled RNA was biotinylated by the click reaction, and biotinylated RNA was purified using streptavidin beads. For quantitative RT-PCR, cDNA was synthesized using the SuperScript VILO cDNA Synthesis Kit (Thermo Fisher Scientific). Quantitative RT-PCR and relative quantification analyses were performed with an MX3000P system (Agilent, Santa Clara, CA) using SYBR Green dye chemistry. All primers are listed in Table S2.

Splicing activity (Fig. 1) was calculated using the following formula:

expression level of CDK6 Ex2-3 junction x 2/ (expression level of CDK6 Ex2 + expression level of CDK6 Ex3).

Plasmid construction

To construct RGS2 Ex1-int4 expression plasmid, the DNA fragment of RGS2 Ex1-int4 was amplified by PCR using cDNA prepared from Pla-B treated cells and the primers RGS2 ATG-Bam for and RGS2 int4STOP-Xho rev. The PCR product was digested with *Bam* HI and *Xho* I and subcloned into pcDNA3.1/Myc-HIS. To construct TBX3 Ex1-int1 expression plasmid, the DNA fragment of TBX3 Ex1-int1 was amplified by PCR using cDNA prepared from Pla-B treated cells and the primers TBX3 ATG-HdIII for and TBX3 int1STOP-Xho rev. The PCR product was digested with *Hin*dIII and *Xho* I and subcloned into pcDNA3.1/Myc-HIS. PCR was performed using PrimeSTAR DNA Polymerase (TaKaRa) according to the manufacturer's instructions. Plasmid

transfection was performed using Lipofectamine 3000 Reagent (Thermo Fisher Scientific) according to the manufacturer's instructions.

Immunoblotting

Cells were directly lysed on plates with 1× SDS-PAGE sample buffer. Proteins were then separated by SDS-PAGE. After electrophoresis, the proteins were transferred onto a PVDF membrane by electroblotting. Following incubation of the membrane with primary and secondary antibodies using standard techniques, protein bands were detected using a NOVEX ECL Chemiluminescent Substrate Reagent Kit (Thermo Fisher Scientific) on an ImageQuant LAS 4000mini (GE Healthcare).

Stable cell line establishment

To establish HeLa cells expressing Flag-p27 FL or Flag-p27* under the control of tetracycline, a DNA fragment of GFP was amplified by PCR from pcDNA6.2 emGFP using GFP Hind III-Eco RI F and GFP ATTTA R primers. The PCR product was digested with EcoRI and KpnI, and subcloned into pTRE3G-BI (TaKaRa Bio) to construct pTRE3G-BI-GFP. The DNA fragments of Flag-p27 FL and Flag-p27* were amplified from Flag-p27 and Flag-p27* plasmids[19], respectively. To amplify Flag-p27, FLAG Hind III-Bgl II F and hp27 cloning R primers were used. To amplify Flag-p27*, FLAG Hind III-Bgl II F and hp27* cloning R primers were used. The PCR products were digested with BglII and NotI, and subcloned into pTRE3G-BI-GFP to construct pTRE3G-BI-GFP-FLAG-p27 FL and pTRE3G-BI-GFP-FLAG-p27*. HeLa Tet On 3G cells (TaKaRa Bio) were transfected with pTRE3G-BI-GFP-FLAG-p27 FL or pTRE3G-BI-GFP-FLAG-p27*, and stable clones were selected by puromycin (1 μg/ml) treatment followed by clonal selection. The primers used for plasmid construction are listed in Table S2.

Stable clones were grown in medium containing Tet system-approved fetal bovine serum (TaKaRa Bio), puromycin and G418. To induce expression, cells were treated for the indicated times with doxycycline (2 μg/ml).

siRNA transfection

Silencer select p27/CDKN1B siRNA (s2837 cat# 4390824) was purchased from Thermo Fisher Scientific. siGENOME Control Pool Non-Targeting #2 (cat# D-001206-14-20) was purchased from GE Healthcare. siRNA transfection was performed using Lipofectamine RNAiMAX (Thermo Fisher Scientific), according to the manufacturer's instructions.

Immunoprecipitation

Cells were suspended in lysis buffer [25 mM HEPES, pH 7.5, 150 mM NaCl, 2 mM $MgCl_2$, 1 mM EDTA, 2.5 mM EGTA, 1% Nonidet P-40, 10% glycerol, cOmplete Protease Inhibitor cocktail (Sigma-Aldrich), and PhosSTOP (Sigma-Aldrich)] and sonicated for 15 s, then incubated on ice for 15 min. After centrifugation, cell extracts were incubated with each primary antibody for 1 h at 4°C with gentle agitation and then with Dynabeads Protein G (Thermo Fisher Scientific) for another 1 h. The beads were washed three times with lysis buffer, and then the bound proteins were extracted with 1× SDS-PAGE sample buffer by heating at 95°C for 5 min.

For ubiquitylated proteins purification, cells were suspended in lysis buffer [25 mM HEPES, pH 7.5, 150 mM NaCl, 2 mM $MgCl_2$, 1 mM EDTA, 2.5 mM EGTA, 1% Nonidet P-40, 10% glycerol, cOmplete Protease Inhibitor cocktail (Sigma-Aldrich), PhosSTOP (Sigma-Aldrich), and 1 mM N−ethylmaleimide (Nakarai tesque, Kyoto, Japan)] and sonicated for 15 s, then incubated on ice for 15 min. After centrifugation, cell extracts were incubated with Agarose-TUBE2 (LifeSensors, Malvern, PA, USA) at 4°C for 4 h with gentle agitation. The beads were washed three times with

lysis buffer, and then the bound proteins were extracted with 1× SDS-PAGE sample buffer by heating at 95°C for 5 min.

In vitro kinase assay

HEK293T cells were transfected with vector, Flag-p27, or Flag-p27* plasmids[19] using Lipofectamine 3000 Reagent, according to the manufacturer's instructions. Lysates of the transfected cells were prepared using lysis buffer (20 mM HEPES-KCl pH 7.4, 150 mM NaCl, 2 mM EDTA, 1% Triton, and cOmplete Protease Inhibitor cocktail). Flag-tagged proteins were purified from the cell lysates using a DDDDK-tagged protein purification kit (MBL), according to the manufacturer's instructions. To check the purification efficiency, the purified proteins were separated by SDS-PAGE, stained with Oriole Fluorescent Gel Stain (Bio-Rad), according to the manufacturer's instructions, and analysed by immunoblotting. The *in vitro* kinase assay was performed using the Cyclin A2/Cdk1 Kinase Enzyme System (Promega, Madison, WI, USA), recombinant Cyclin B1/Cdk1 (SignalChem Biotech Inc., Richmond, BC, Canada), and ADP-Glo kinase assay (Promega), according to the manufacturers' instructions. Briefly, the kinase complex was mixed with the purified Flag-tagged proteins and then incubated at 25°C for 10 min. Histone H1 and ATP were added to the reaction, followed by incubation at 25°C for 1 h. ADP-Glo Reagent was added to the reaction, followed by incubation at 25°C for 40 min. Kinase Detection Reagent was added to the reaction, followed by incubation at 25°C for 30 min. Luminescence was measured using a Varioskan Flash (Thermo Fisher Scientific).

Analysis of NGS data

We reanalyzed our previous data (NCBI accession number GSE72156) [53] and calculated the number of amino acids when pre-mRNA is translated from the start codon to the inflame stop codon in the

introns affected by splicing inhibition. We also performed a gene ontology analysis using AmiGO 2 to select cell cycle regulators [62-64].

Acknowledgments

We are grateful to Ms. K. Komori and Mr. K. Kikuchi for technical assistance. We thank Dr. Y. Yoshida (Tokyo Metropolitan Institute of Medical Science) for HA-Skp2 plasmid. We also thank Drs. N. Kataoka and K Fukumura for critical reading of the manuscript. This research was funded by JSPS KAKENHI (JP21H02423), Takeda Science Foundation, Tamura Science & Technology Foundation, the Kato Memorial Bioscience Foundation, The Ichiro Kanehara Foundation, and Suzuken Memorial Foundation.

References

1. Grzybowska, E.A. Human intronless genes: functional groups, associated diseases, evolution, and mRNA processing in absence of splicing. *Biochem Biophys Res Commun* **424**, 1-6 (2012).
2. Wahl, M.C., Will, C.L. & Luhrmann, R. The spliceosome: design principles of a dynamic RNP machine. *Cell* **136**, 701-18 (2009).
3. Papasaikas, P. & Valcarcel, J. The Spliceosome: The Ultimate RNA Chaperone and Sculptor. *Trends Biochem Sci* **41**, 33-45 (2016).
4. Chhipi-Shrestha, J.K. et al. Splicing modulators elicit global translational repression by condensate-prone proteins translated from introns. *Cell Chem Biol* (2021).
5. Quesada, V. et al. Exome sequencing identifies recurrent mutations of the splicing factor SF3B1 gene in chronic lymphocytic leukemia. *Nat Genet* **44**, 47-52 (2011).
6. Rossi, D. et al. Mutations of the SF3B1 splicing factor in chronic lymphocytic leukemia: association with progression and fludarabine-refractoriness. *Blood* **118**, 6904-8 (2011).
7. Wang, L. et al. SF3B1 and other novel cancer genes in chronic lymphocytic leukemia. *N Engl J Med* **365**, 2497-506 (2011).
8. Yoshida, K. et al. Frequent pathway mutations of splicing machinery in myelodysplasia. *Nature* **478**, 64-9 (2011).
9. Cooper, T.A., Wan, L. & Dreyfuss, G. RNA and disease. *Cell* **136**, 777-93 (2009).
10. Bousquet-Antonelli, C., Presutti, C. & Tollervey, D. Identification of a regulated pathway for nuclear pre-mRNA turnover. *Cell* **102**, 765-75 (2000).
11. Dziembowski, A. et al. Proteomic analysis identifies a new complex required for nuclear pre-mRNA retention and splicing. *EMBO J* **23**, 4847-56 (2004).
12. Galy, V. et al. Nuclear retention of unspliced mRNAs in yeast is mediated by perinuclear Mlp1. *Cell* **116**, 63-73 (2004).
13. Rutz, B. & Seraphin, B. A dual role for BBP/ScSF1 in nuclear pre-mRNA retention and splicing. *EMBO J* **19**, 1873-86 (2000).
14. Kurosaki, T., Popp, M.W. & Maquat, L.E. Quality and quantity control of gene expression by nonsense-mediated mRNA decay. *Nat Rev Mol Cell Biol* **20**, 406-420 (2019).
15. Kaida, D. et al. Spliceostatin A targets SF3b and inhibits both splicing and nuclear retention of pre-mRNA. *Nat Chem Biol* **3**, 576-83 (2007).
16. Mizui, Y. et al. Pladienolides, new substances from culture of Streptomyces platensis Mer-

11107. III. In vitro and in vivo antitumor activities. *J Antibiot (Tokyo)* **57**, 188-96 (2004).

17. Nakajima, H. et al. New antitumor substances, FR901463, FR901464 and FR901465. II. Activities against experimental tumors in mice and mechanism of action. *J Antibiot (Tokyo)* **49**, 1204-11 (1996).
18. Kotake, Y. et al. Splicing factor SF3b as a target of the antitumor natural product pladienolide. *Nat Chem Biol* **3**, 570-5 (2007).
19. Satoh, T. & Kaida, D. Upregulation of p27 cyclin-dependent kinase inhibitor and a C-terminus truncated form of p27 contributes to G1 phase arrest. *Sci Rep* **6**, 27829 (2016).
20. Kikuchi, K. & Kaida, D. CCNE1 and E2F1 Partially Suppress G1 Phase Arrest Caused by Spliceostatin A Treatment. *Int J Mol Sci* **22**(2021).
21. Hochegger, H., Takeda, S. & Hunt, T. Cyclin-dependent kinases and cell-cycle transitions: does one fit all? *Nat Rev Mol Cell Biol* **9**, 910-6 (2008).
22. Lim, S. & Kaldis, P. Cdks, cyclins and CKIs: roles beyond cell cycle regulation. *Development* **140**, 3079-93 (2013).
23. Furuno, N., den Elzen, N. & Pines, J. Human cyclin A is required for mitosis until mid prophase. *J Cell Biol* **147**, 295-306 (1999).
24. Lindqvist, A., Rodriguez-Bravo, V. & Medema, R.H. The decision to enter mitosis: feedback and redundancy in the mitotic entry network. *J Cell Biol* **185**, 193-202 (2009).
25. Ohi, R. & Gould, K.L. Regulating the onset of mitosis. *Curr Opin Cell Biol* **11**, 267-73 (1999).
26. den Elzen, N. & Pines, J. Cyclin A is destroyed in prometaphase and can delay chromosome alignment and anaphase. *J Cell Biol* **153**, 121-36 (2001).
27. Erlandsson, F., Linnman, C., Ekholm, S., Bengtsson, E. & Zetterberg, A. A detailed analysis of cyclin A accumulation at the G(1)/S border in normal and transformed cells. *Exp Cell Res* **259**, 86-95 (2000).
28. Geley, S. et al. Anaphase-promoting complex/cyclosome-dependent proteolysis of human cyclin A starts at the beginning of mitosis and is not subject to the spindle assembly checkpoint. *J Cell Biol* **153**, 137-48 (2001).
29. Pines, J. & Hunter, T. Human cyclin A is adenovirus E1A-associated protein p60 and behaves differently from cyclin B. *Nature* **346**, 760-3 (1990).
30. Yam, C.H., Fung, T.K. & Poon, R.Y. Cyclin A in cell cycle control and cancer. *Cell Mol Life Sci* **59**, 1317-26 (2002).
31. Acquaviva, C. & Pines, J. The anaphase-promoting complex/cyclosome: APC/C. *J Cell Sci* **119**, 2401-4 (2006).

32. Fung, T.K. & Poon, R.Y. A roller coaster ride with the mitotic cyclins. *Semin Cell Dev Biol* **16**, 335-42 (2005).
33. van Leuken, R., Clijsters, L. & Wolthuis, R. To cell cycle, swing the APC/C. *Biochim Biophys Acta* **1786**, 49-59 (2008).
34. McGowan, C.H. & Russell, P. Human Wee1 kinase inhibits cell division by phosphorylating p34cdc2 exclusively on Tyr15. *EMBO J* **12**, 75-85 (1993).
35. Norbury, C., Blow, J. & Nurse, P. Regulatory phosphorylation of the p34cdc2 protein kinase in vertebrates. *EMBO J* **10**, 3321-9 (1991).
36. Gautier, J., Solomon, M.J., Booher, R.N., Bazan, J.F. & Kirschner, M.W. cdc25 is a specific tyrosine phosphatase that directly activates p34cdc2. *Cell* **67**, 197-211 (1991).
37. Sherr, C.J. & Roberts, J.M. CDK inhibitors: positive and negative regulators of G1-phase progression. *Genes Dev* **13**, 1501-12 (1999).
38. Toyoshima, H. & Hunter, T. p27, a novel inhibitor of G1 cyclin-Cdk protein kinase activity, is related to p21. *Cell* **78**, 67-74 (1994).
39. Hengst, L. & Reed, S.I. Translational control of p27Kip1 accumulation during the cell cycle. *Science* **271**, 1861-4 (1996).
40. Nakayama, K. et al. Skp2-mediated degradation of p27 regulates progression into mitosis. *Dev Cell* **6**, 661-72 (2004).
41. Kaufmann, S.H., Desnoyers, S., Ottaviano, Y., Davidson, N.E. & Poirier, G.G. Specific proteolytic cleavage of poly(ADP-ribose) polymerase: an early marker of chemotherapy-induced apoptosis. *Cancer Res* **53**, 3976-85 (1993).
42. Chen, J. The Cell-Cycle Arrest and Apoptotic Functions of p53 in Tumor Initiation and Progression. *Cold Spring Harb Perspect Med* **6**, a026104 (2016).
43. Matlashewski, G., Banks, L., Pim, D. & Crawford, L. Analysis of human p53 proteins and mRNA levels in normal and transformed cells. *Eur J Biochem* **154**, 665-72 (1986).
44. Scheffner, M., Werness, B.A., Huibregtse, J.M., Levine, A.J. & Howley, P.M. The E6 oncoprotein encoded by human papillomavirus types 16 and 18 promotes the degradation of p53. *Cell* **63**, 1129-36 (1990).
45. Cretu, C. et al. Structural basis of intron selection by U2 snRNP in the presence of covalent inhibitors. *Nat Commun* **12**, 4491 (2021).
46. Koga, M., Hayashi, M. & Kaida, D. Splicing inhibition decreases phosphorylation level of Ser2 in Pol II CTD. *Nucleic Acids Res* **43**, 8258-67 (2015).
47. Koga, M. et al. U2 snRNP is required for expression of the 3' end of genes. *PLoS One* **9**,

e98015 (2014).

48. Muraoka, S. et al. Rbm38 Reduces the Transcription Elongation Defect of the SMEK2 Gene Caused by Splicing Deficiency. *Int J Mol Sci* **21**(2020).
49. Girard, C. et al. Post-transcriptional spliceosomes are retained in nuclear speckles until splicing completion. *Nat Commun* **3**, 994 (2012).
50. Wang, C. et al. Phosphorylation of spliceosomal protein SAP 155 coupled with splicing catalysis. *Genes Dev* **12**, 1409-14 (1998).
51. Cadart, C., Zlotek-Zlotkiewicz, E., Le Berre, M., Piel, M. & Matthews, H.K. Exploring the function of cell shape and size during mitosis. *Dev Cell* **29**, 159-69 (2014).
52. Morla, A.O., Draetta, G., Beach, D. & Wang, J.Y. Reversible tyrosine phosphorylation of cdc2: dephosphorylation accompanies activation during entry into mitosis. *Cell* **58**, 193-203 (1989).
53. Yoshimoto, R. et al. Global analysis of pre-mRNA subcellular localization following splicing inhibition by spliceostatin A. *RNA* **23**, 47-57 (2017).
54. Montagnoli, A. et al. Ubiquitination of p27 is regulated by Cdk-dependent phosphorylation and trimeric complex formation. *Genes Dev* **13**, 1181-9 (1999).
55. Yoshida, Y. et al. A comprehensive method for detecting ubiquitinated substrates using TR-TUBE. *Proc Natl Acad Sci U S A* **112**, 4630-5 (2015).
56. Hjerpe, R. et al. Efficient protection and isolation of ubiquitylated proteins using tandem ubiquitin-binding entities. *EMBO Rep* **10**, 1250-8 (2009).
57. Lander, E.S. et al. Initial sequencing and analysis of the human genome. *Nature* **409**, 860-921 (2001).
58. Nakajima, H. et al. New antitumor substances, FR901463, FR901464 and FR901465. I. Taxonomy, fermentation, isolation, physico-chemical properties and biological activities. *J Antibiot (Tokyo)* **49**, 1196-203 (1996).
59. Seiler, M. et al. H3B-8800, an orally available small-molecule splicing modulator, induces lethality in spliceosome-mutant cancers. *Nat Med* **24**, 497-504 (2018).
60. Hong, D.S. et al. A phase I, open-label, single-arm, dose-escalation study of E7107, a precursor messenger ribonucleic acid (pre-mRNA) splicesome inhibitor administered intravenously on days 1 and 8 every 21 days to patients with solid tumors. *Invest New Drugs* **32**, 436-44 (2014).
61. Shumilov, E. et al. Current status and trends in the diagnostics of AML and MDS. *Blood Rev* **32**, 508-519 (2018).

62. Ashburner, M. et al. Gene ontology: tool for the unification of biology. The Gene Ontology Consortium. *Nat Genet* **25**, 25-9 (2000).

63. Carbon, S. et al. AmiGO: online access to ontology and annotation data. *Bioinformatics* **25**, 288-9 (2009).

64. Gene Ontology, C. The Gene Ontology resource: enriching a GOld mine. *Nucleic Acids Res* **49**, D325-D334 (2021).

Figure legends

Figure 1. Pla-B treatment causes G2/M phase arrest and cell death. (A, B) HeLa S3 cells were treated with MeOH or the indicated concentrations of Pla-B. The number of cells (A) and cell viability (B) were analysed at the indicated time points. (C, D) HeLa S3 cells were treated with the indicated concentrations of Pla-B for the indicated periods and then washed out. The number of cells (C) and cell viability (D) were analysed at the indicated time points. Red and black triangles in (C) indicate the time point of Pla-B washout and cell harvest, respectively. (E, F) HeLa S3 cells were treated with the indicated concentrations of Pla-B for the indicated periods and then washed out. Forty-eight hours after the addition of Pla-B, newly transcribed RNAs were labelled for 1 h and then analysed by RT-qPCR. Splicing activity was calculated based on the relative expression levels of CDK6 Ex2, Ex2-3 junction and Ex3 in Fig. S2 (E). Forty-eight hours after the addition of Pla-B, protein samples were prepared and analysed by immunoblotting using the indicated antibodies. The arrow heads indicates phosphorylated SF3B1 (F). Statistical significance was assessed by the one-way ANOVA and Dunnett's test (*: $P < 0.05$; **: $P < 0.01$; ***: $P < 0.01$). Error bars indicate s.d. (n = 3).

Figure 2. CHX suppresses G2/M phase arrest and cell death caused by Pla-B. (A, B) HeLa S3 cells were treated with 10 ng/ml Pla-B, 3 μg/ml Act D, or 10 μg/ml CHX. The number of cells (A) and cell viability (B) were analysed at the indicated time points. Statistical significance was assessed by the one-way ANOVA and Dunnett's test (*: $P < 0.05$; ***: $P < 0.01$). (C) HeLa S3 cells were treated with 10 ng/ml Pla-B or 10 μg/ml CXH and cell cycle was analysed by cytometry. Statistical significance was assessed by the two-tailed t-test (**$P < 0.01$). (D) HeLa S3 cells were treated with the indicated concentrations of Pla-B and CHX. Cell viability were analysed at 72 h. Statistical

significance was assessed by the two-tailed t-test (*: $P < 0.05$; **$P < 0.01$). (E) HeLa S3 cells were treated with the indicated concentrations of Pla-B and CHX. Cell cycle was analyzed at 24 h by cytometry. Statistical significance was assessed by the two-tailed t-test (**$P < 0.01$). Error bars indicate s.d. (n = 3).

Figure 3. Low doses of Pla-B cause M phase arrest and high doses of Pla-B cause G2 phase arrest. (A-D) Two hours after release from a double thymidine block (DTB), synchronized HeLa S3 cells were treated with MeOH or the indicated concentrations of Pla-B. Black triangles indicate the time points of cell harvest and sample preparation (A). Cell cycle was analyzed at the indicated time points by cytometry (B). Morphology of the cells was observed under a microscope and round cells were counted at the indicated time points (C). Protein samples were prepared at the indicated time points. The protein levels of indicated proteins and phosphorylation status of Cdk1 were analysed by immunoblotting. Protein levels of α-tubulin were analysed as an internal control (D). Error bars indicate s.d. (n = 3).

Figure 4. Overexpression of p27* causes partial G2 phase arrest. (A–C) Cells expressing Flag-p27* under the control of tetracycline were synchronized by a double thymidine block. The cells were treated with 2 μg/ml doxycycline (Dox) or DMSO (Control) at the same time as the second thymidine treatment. After release from the double thymidine block, the protein levels of indicated proteins were analysed by immunoblotting (A). Cell cycle was analysed by cytometry (B). The morphology of the cells was observed, and the number of round cells was counted at 20 h after release from the double thymidine block (C). (D) Eighteen hours after treatment with thymidine, synchronized HeLa S3 cells were transfected with control or p27 siRNA. Two hours after release from the second thymidine block, the cells were treated with MeOH or indicated concentration of

Pla-B and cultured for an additional 6 h, and then analysed by immunoblotting. (E, F) HeLa S3 cells were treated with thymidine, siRNA, and MeOH or Pla-B as described in (D). Cell cycle was analyzed by cytometoty at 8 or 12 h after release from the double thymidine block (E). The morphology of the cells was observed and round cells were counted at 12 h after release from the double thymidine block (F). Error bars indicate s.d. (n = 3).

Figure 5. p27* binds to and inhibits M phase Cyclin. (A) Cells expressing Flag-p27* under the control of tetracycline were synchronized by a double thymidine block. The cells were treated with 1 μg/ml DOX at the same time as release from the double thymidine block. The cells were harvested at 8 h after release from the double thymidine block (G2/M phase) and then immunoprecipitation was performed using anti-DDDDK (Flag) antibodies. Flag-tagged and coimmunoprecipitated proteins were analysed by immunoblotting. (B, C) Purified Flag-tagged proteins were applied to an *in vitro* kinase assay reaction and kinase activities of Cyclin A2/Cdk1 (B) and Cyclin B1/Cdk1 (C) were measured. Statistical significance was assessed by the one-way ANOVA and Dunnett's test (*: $P < 0.05$; **: $P < 0.01$; ***: $P < 0.01$). Error bars indicate s.d. (n = 3).

Figure 6. p27* is a stable protein with cell cycle inhibitory activity. (A) Two hours after release from a double thymidine block, synchronized HeLa S3 cells were treated with MeOH or the indicated concentrations of Pla-B. The cells were harvested at 8 h after release from the double thymidine block (G2/M phase) and total RNA was purified. Splicing pattern changes were analysed by RT-PCR. (B) Cells expressing Flag-p27 FL or Flag-p27* under the control of tetracycline were synchronized by a double thymidine block. The cells were treated with 1 μg/ml DOX at the same time as release from the double thymidine block. Four hours after release from the double thymidine block, the cells were treated with 20 μM MG132. Eight hours after release from the double thymidine block, protein levels

of indicated proteins were analysed by immunoblotting. (C) Two hours after release from a double thymidine block, synchronized HeLa S3 cells were treated with MeOH or 10 ng/ml Pla-B. Six hours after release from the double thymidine block, the cells were treated with 20 μM MG132. Eight hours after release from the double thymidine block, protein levels of indicated proteins were analysed by immunoblotting. (D) HeLa S3 cells were transfected with HA-Skp2 and Flag-p27 FL or Flag-p27* and then treated with 20 μM MG132 for 4 h. Cell extracts were incubated with Agarose-TUBE for 4 h to purify ubiquitylated proteins. Purified proteins were analysed by immunoblotting. The relative band intensities (p27 FL = 1) were quantified and are shown in the bar graph (right panel). Red rectangles indicate the areas where band intensity was measured. Statistical significance was assessed by the two-tailed t-test (*$P < 0.05$). Error bars indicate s.d. (n = 3). (E) HeLa S3 cells were treated with the 10 ng/ml Pla-B for indicated periods and then washed out. Protein levels of the indicated proteins were analyzed by immunoblotting at 72 h. (F) HeLa S3 cells were treated with the 10 ng/ml Pla-B for 8 h and then washed out. The number of cells were analysed at the indicated time points. Statistical significance was assessed by the one-way ANOVA and Tukey's test. Error bars indicate s.d. (n = 7).

Figure S1. Pla-B treatment causes cell cycle arrest and apoptosis. (A) HeLa S3 cells were treated with the indicated concentrations of Pla-B and protein levels of indicated proteins were analyzed by immunoblotting at the indicated time points. (B-D) MDA-MB-231 cells and MCF7 cells were treated with indicated concentrations of Pla-B for indicated periods. The number of cells (B) and cell viability (C) were analysed. Protein levels of indicated proteins were analyzed by immunoblotting (D). Error bars indicate s.d. (n = 3)

Figure S2. Splicing activity is recovered after washout of Pla-B. (A, B) HeLa S3 cells were treated with the indicated concentrations of Pla-B for the indicated periods and then washed out. Forty-eight hours after the addition of Pla-B, newly transcribed RNAs were labelled for 1 h and then analysed by RT-qPCR. Error bars indicate s.d. (n = 3).

Figure S3. Pla-B treatment causes G2/M phase arrest. Two hours after release from a double thymidine block, synchronized HeLa S3 cells were treated with the indicated concentrations of Pla-B and cell cycle was analyzed at the indicated time points by cytometry. Error bars indicate s.d. (n = 3).

Figure S4. Low doses of Pla-B cause M phase arrest and high doses of Pla-B cause G2 phase arrest. (A, B) Two hours after release from a double thymidine block, synchronized HeLa S3 cells were treated with the indicated concentrations of Pla-B. Morphology of the cells was observed under a microscope and round cells were counted at the indicated time points. Error bars indicate s.d. (n = 3).

Figure S5. p27* is accumulated in G2 arrested cells. Two hours after release from a double thymidine block, synchronized HeLa S3 cells were treated with MeOH or the indicated concentrations of Pla-B. Protein samples were prepared at the indicated time points and the protein levels of indicated proteins and phosphorylation status of Cdk1 were analysed by immunoblotting. Protein levels of α-tubulin were analysed as an internal control.

Figure S6. Pre-mRNAs of RGS2, TBX3 and CDKN1B were accumulated in Pla-B treated cells. Non-synchronized HeLa S3 cells and HeLa S3 cells synchronized at G2/M phase were treated with

MeOH or the indicated concentrations of Pla-B for 8 h. Total RNA was purified and the indicated pre-mRNAs were analyzed by RT-PCR.

Figure S7. p27* overexpression causes cell cycle arrest. (A, B) HeLa S3 cells were transfected with expression plasmid of TBX3 Ex1-Int1, RGS2 Ex1-Int4 or CDKN1B Ex1-Int1 (p27*) and expression of the truncated forms were confirmed by immunoblotting. (C) HeLa S3 cells were treated with the indicated concentrations of Pla-B for 8 h and endogenous proteins were detected using the indicated antibodies by immunoblotting. (D, E) HeLa S3 cells were transfected with expression plasmid of truncated forms of TBX3 Ex1-Int1, RGS2 Ex1-Int4 or CDKN1B Ex1-Int1 (p27*) and the number of cells (D) and cell viability (E) were analysed at the indicated time points. Statistical significance was assessed by the two-tailed t-test (**$P < 0.01$). Error bars indicate s.d. (n = 3).

Figure S8. Purification of Flag-tagged proteins. (A, B) HEK293T cells were transfected with vector, Flag-p27 FL, or Flag-p27* plasmid, and then protein extracts were prepared. Flag-tagged proteins were purified from the protein extracts using an anti-Flag antibody and then eluted using a Flag peptide. The Flag-tagged proteins were analysed by oriole staining (A) and immunoblotting (B). Bovine serum albumin (BSA) was also analysed to estimate the amounts of Flag-tagged proteins.

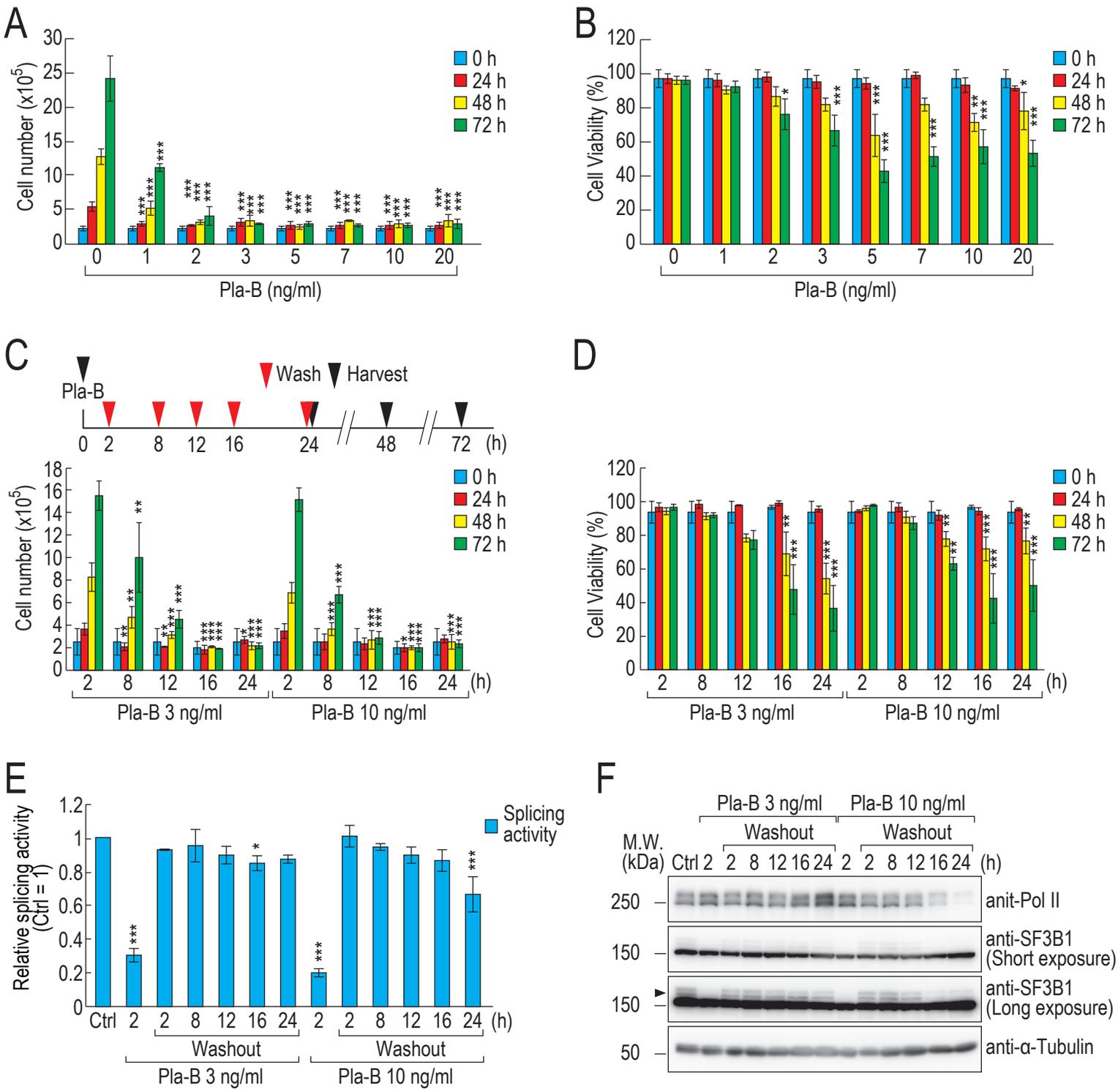

Fig. 1 Kaida et al.

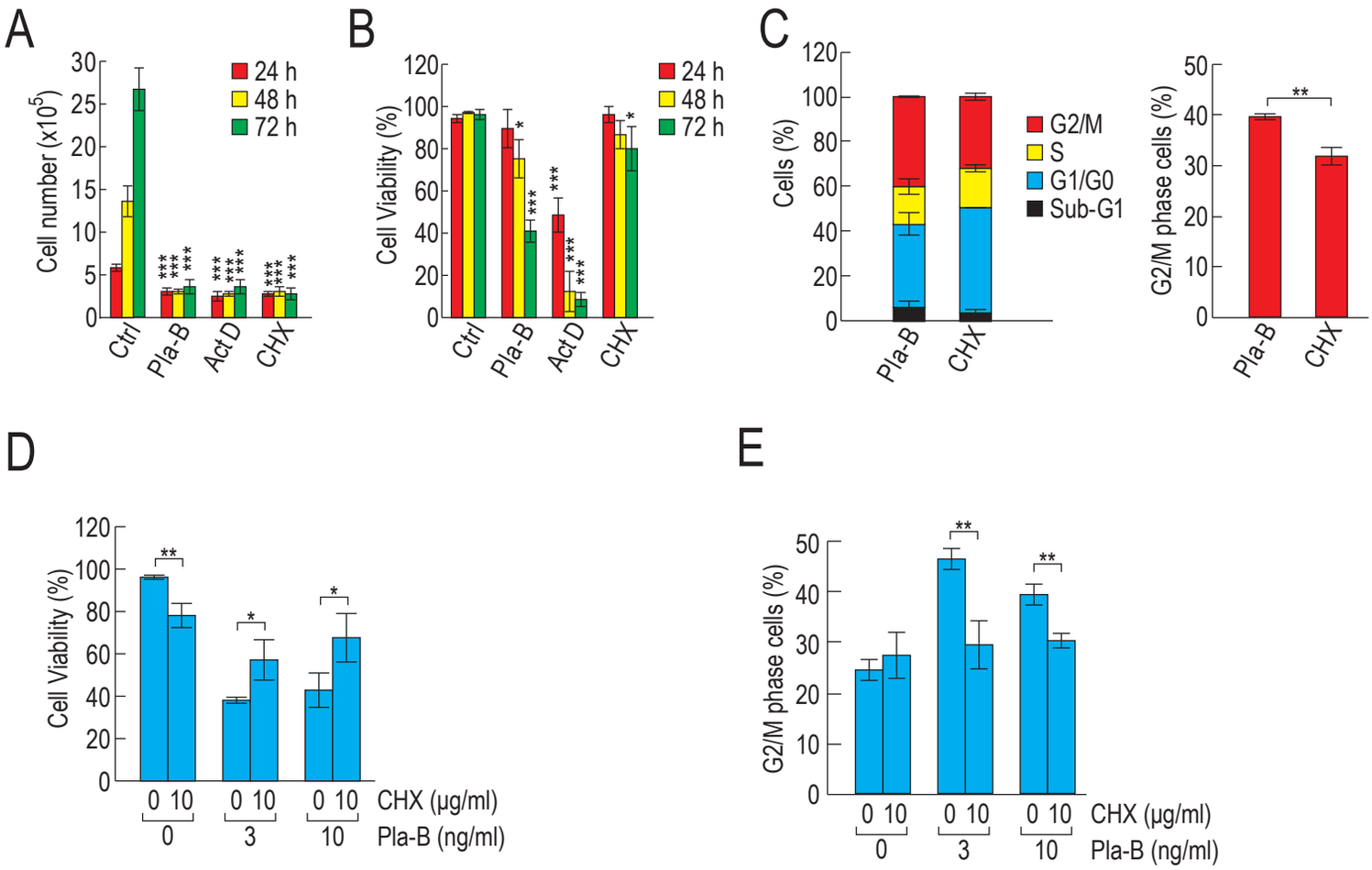

Fig. 2 Kaida et al.

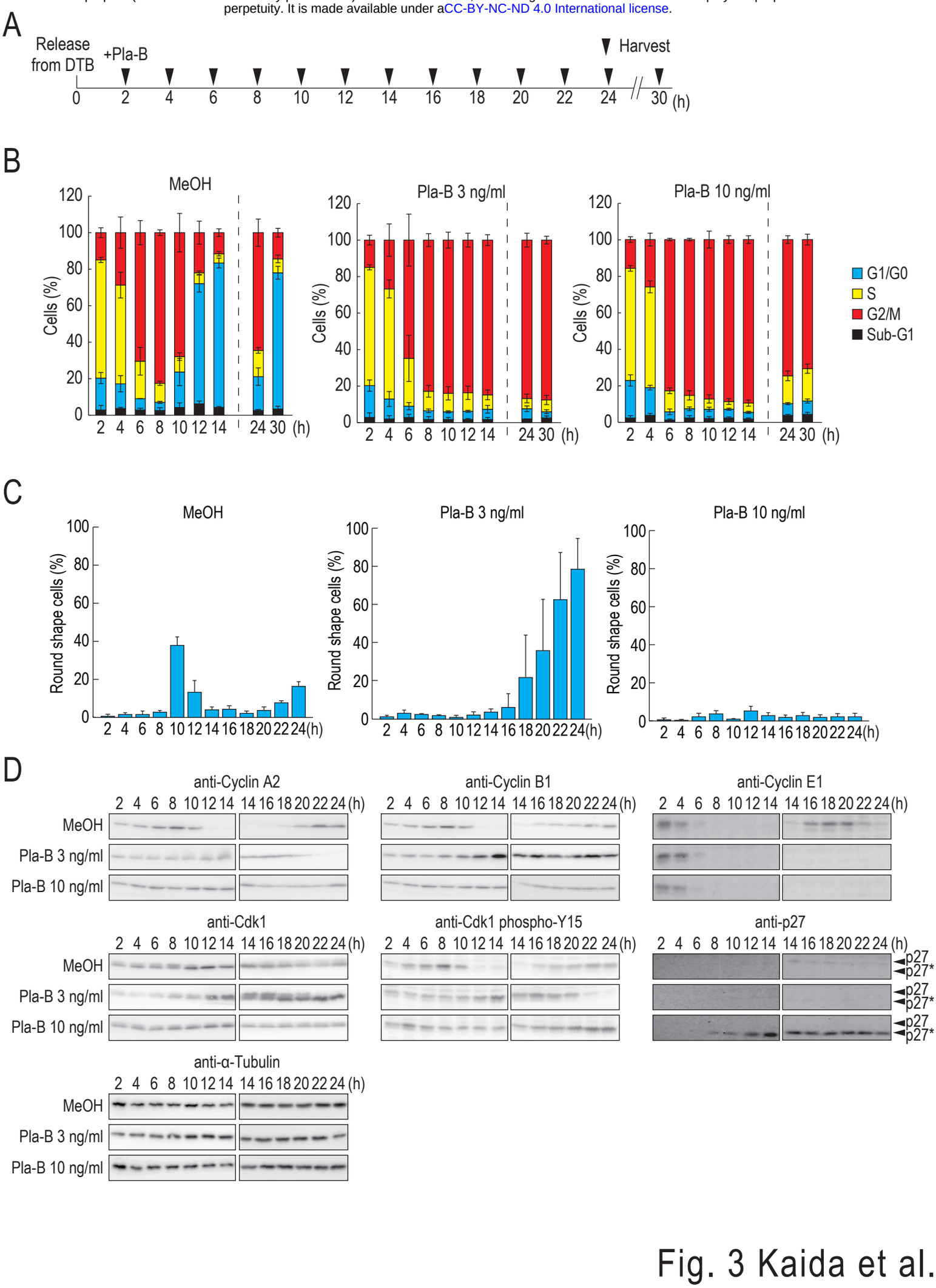

Fig. 3 Kaida et al.

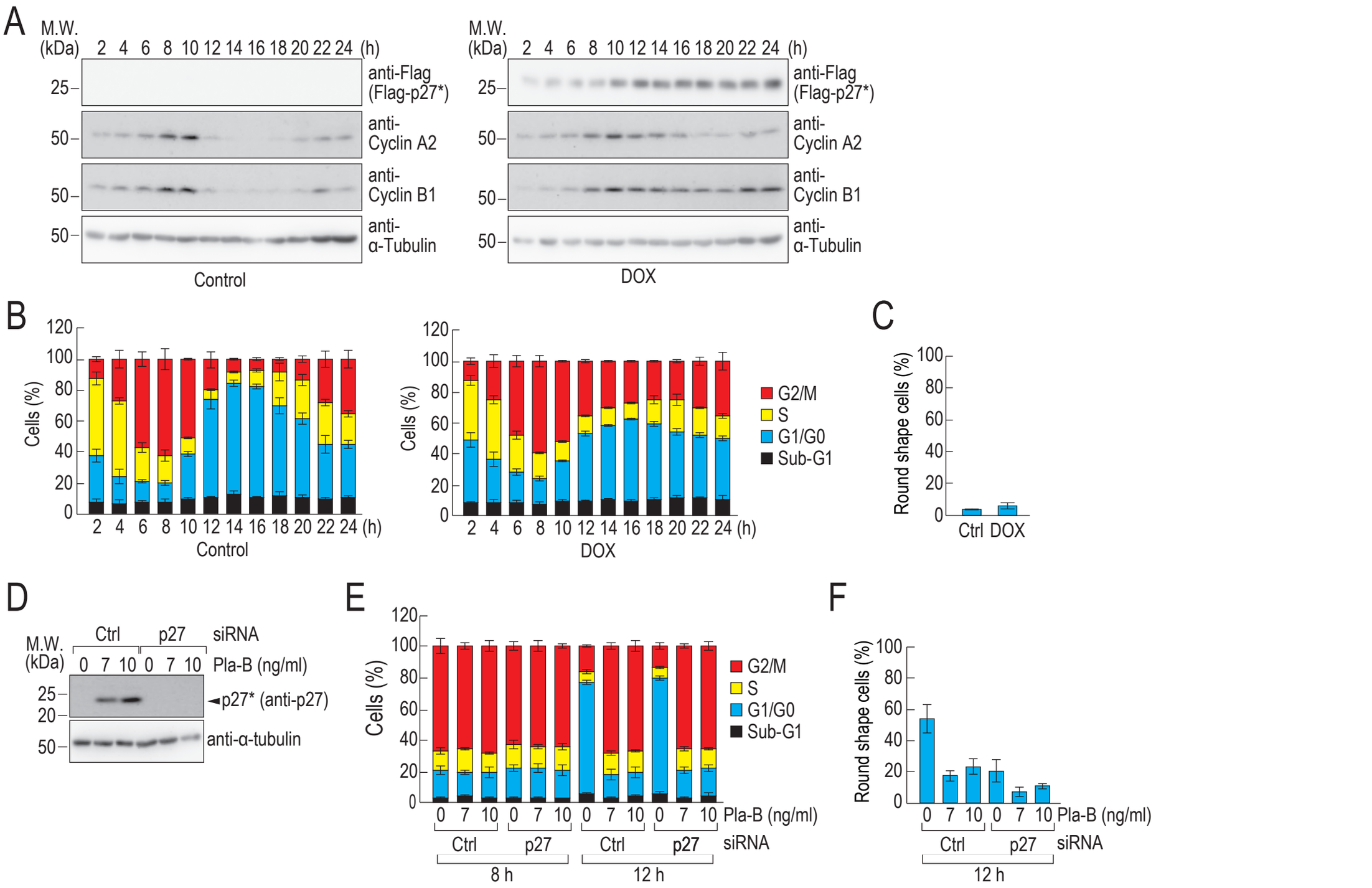

Fig. 4 Kaida et al.

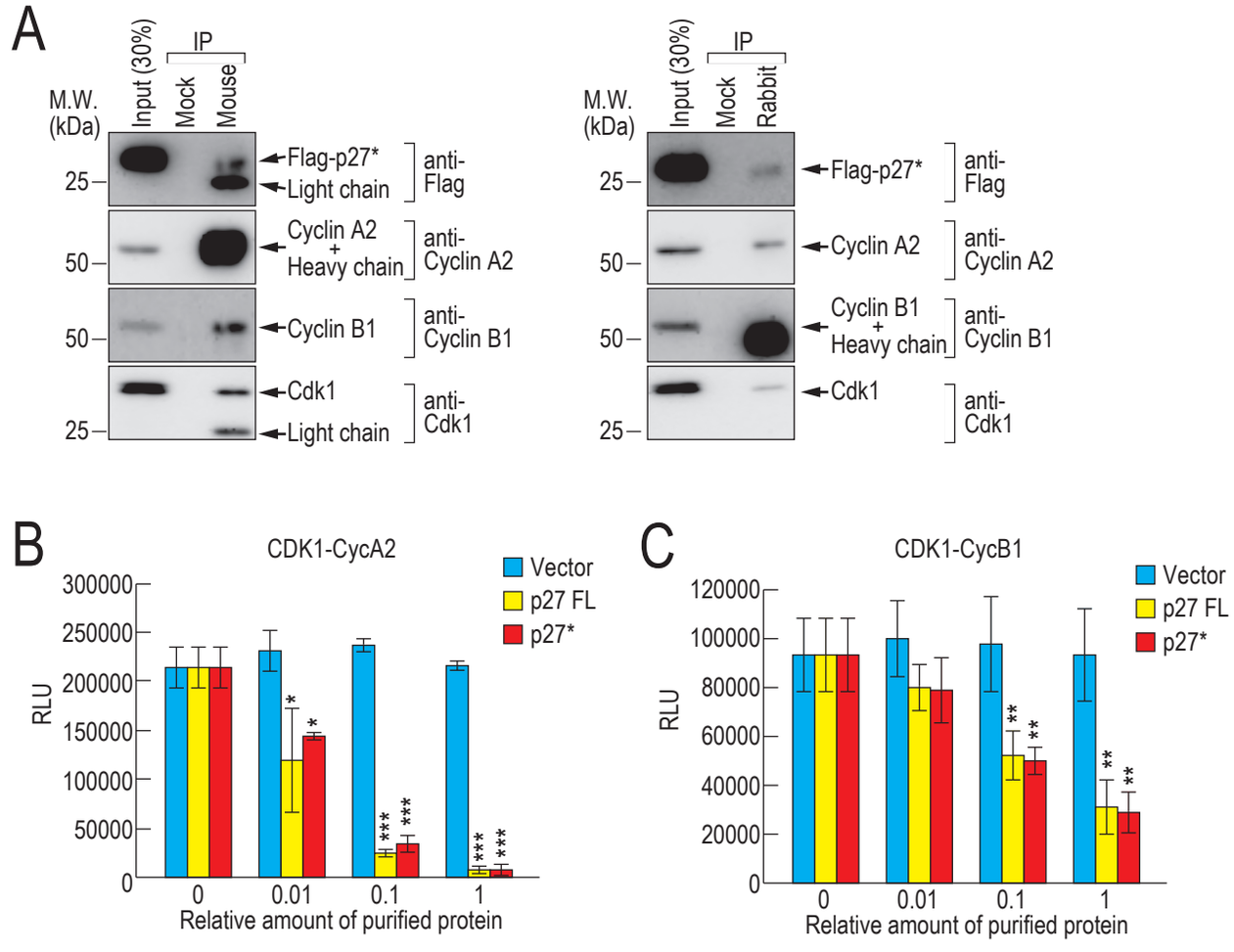

Fig. 5 Kaida et al.

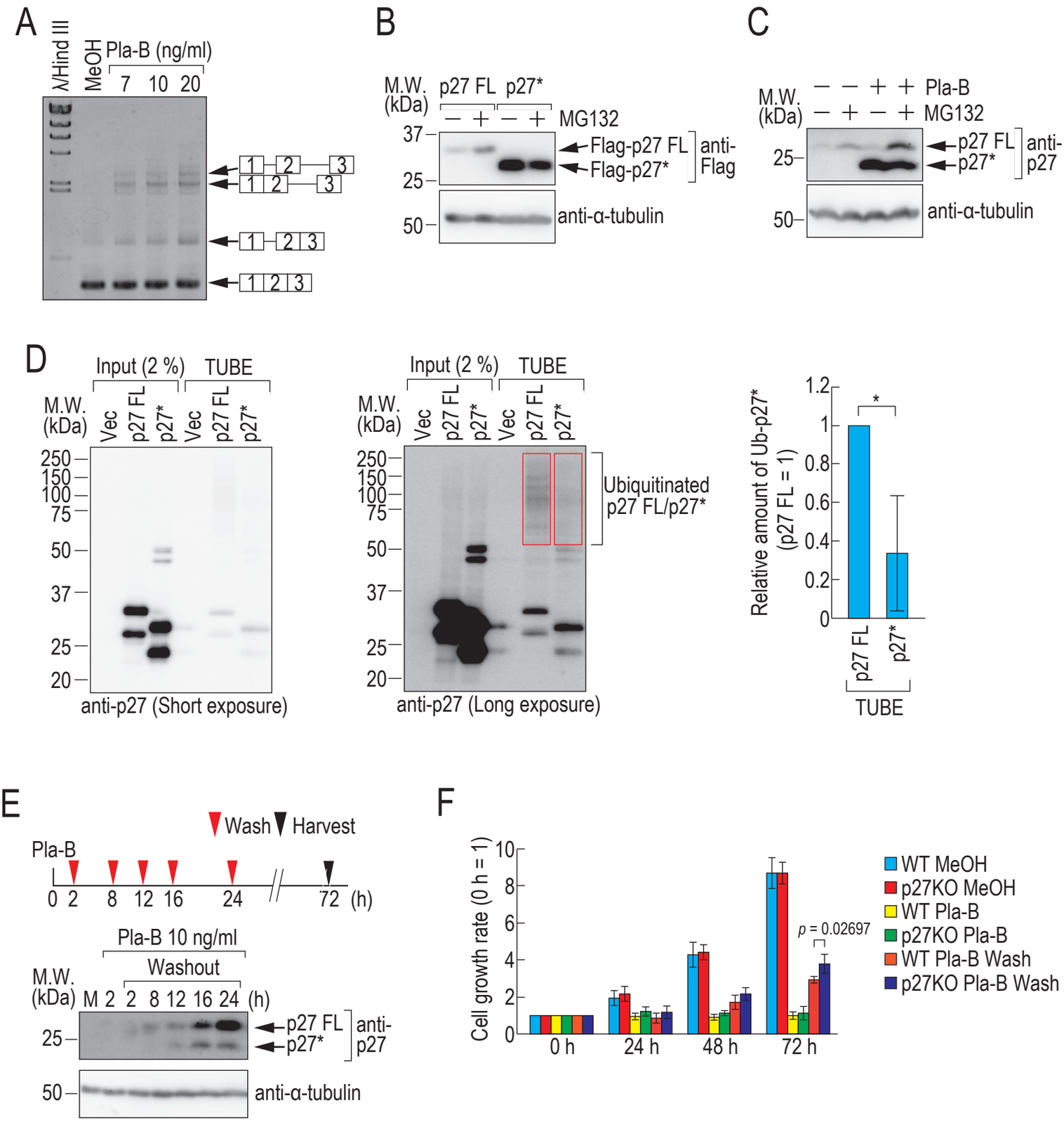

Fig. 6 Kaida et al.